Journal of Medicinal Chemistry

Article

pubs.acs.org/jmc

Development and Characterization of Glutamyl-Protected *N*-Hydroxyguanidines as Reno-Active Nitric Oxide Donor Drugs with Therapeutic Potential in Acute Renal Failure

Qingzhi Zhang,[‡] Philip Milliken,[§] Agnieszka Kulczynska,[‡] Alex M. Z. Slawin,[‡] Adele Gordon,[§] Nicholas S. Kirkby,[§] David J. Webb,[§] Nigel P. Botting,[‡,†] and Ian L. Megson[∥,*]

[‡]EASTChem, School of Chemistry and Centre for Biomolecular Sciences, The University of St. Andrews, North Haugh, St. Andrews KY16 9ST, U.K.

[§]Centre for Cardiovascular Science, The Queen's Medical Research Institute, The University of Edinburgh, 47 Little France Crescent, Edinburgh EH16 4TJ, U.K.

[∥]Free Radical Research Facility, Department of Diabetes and Cardiovascular Science, The University of The Highlands & Islands, Centre for Health Science, Old Perth Road, Inverness IV2 3JH, U.K.

Supporting Information

ABSTRACT: Acute renal failure (ARF) has high mortality and no effective treatment. Nitric oxide (NO) delivery represents a credible means of preventing the damaging effects of vasoconstriction, central to ARF, but design of drugs with the necessary renoselectivity is challenging. Here, we developed *N*-hydroxyguanidine NO donor drugs that were protected against spontaneous NO release by linkage to glutamyl adducts that could be cleaved by γ-glutamyl transpeptidase (γ-GT), found predominantly in renal tissue. Parent NO donor drug activity was optimized in advance of glutamyl adduct prodrug design. A lead compound that was a suitable substrate for γ-GT-mediated deprotection was identified. Metabolism of this prodrug to the active parent compound was confirmed in rat kidney homogenates, and the prodrug was shown to be an active vasodilator in rat isolated perfused kidneys (EC_{50} ~50 μM). The data confirm that glutamate protection of *N*-hydroxyguanidines is an approach that might hold promise in ARF.

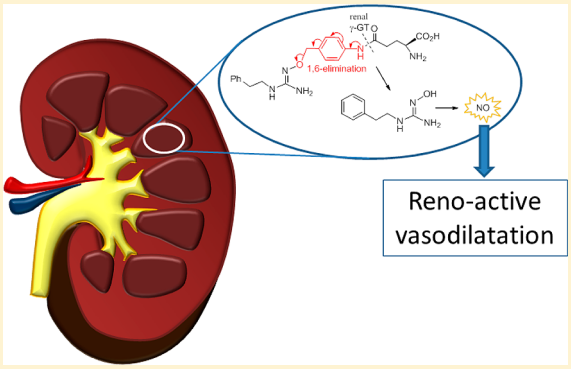

INTRODUCTION

Acute renal failure (ARF) affects ~5% of all hospitalized patients and 10−30% of intensive care patients.[1] Prognosis is poor, with a mortality rate exceeding 50%[2] and only 60−70% of survivors regaining full independence.[3] Ischemia-reperfusion injury is the most common cause of ARF, but sepsis, hypotension, and nephrotoxic drugs are also important.[4] Aortic cross-clamping during cardiopulmonary bypass surgery is a major cause of ischemic ARF, although acute changes in cardiac output due to myocardial infarction or ventricular fibrillation can also underpin poor renal perfusion, leading to organ failure.[5] Renal replacement therapy is the only recognized treatment for ARF;[6] pharmacological interventions, including low dose dopamine,[7−9] dopexamine (synthetic dopamine analogue),[10−12] mannitol/loop diuretics,[13−15] calcium entry blockers,[16] anaritide (atrial natriuretic peptide),[17] and *N*-acetylcysteine,[18,19] have all failed to show reproducible clinical benefits. This highlights the need for effective therapies to treat ARF and to reduce the reliance on costly renal replacement therapy, and the challenges linked to achieving this goal.

Oxidative stress due to mitochondrial dysfunction and xanthine oxidase (XO; EC 1.17.3.2) activation in the immediate aftermath of ischemia-reperfusion, exacerbated by reactive oxygen species (ROS) production from infiltrating inflammatory cells, is key to the etiology of ARF.[20] ROS have multiple deleterious effects, but rapid reaction with the endogenous vasodilator, antithrombotic, and anti-inflammatory agent, nitric oxide (NO),[21,22] is a crucial component, not only because of the loss of the highly beneficial effects of NO[20,23,24] but also through generation of nephrotoxic peroxynitrite ($ONOO^-$) as the product of the reaction.[25] Endogenous NO is synthesized from L-arginine (L-Arg) and oxygen by NO synthase (NOS) enzymes and is critical in regulating renal perfusion and glomerular hemodynamics under basal conditions.[26] NO is protective against ARF and increased NO synthesis from endothelial and neuronal NOS (eNOS, nNOS) is beneficial in ischemia:[27] NOS inhibition decreases NO production, further reducing renal function in ischemic ARF in rats.[28,29] These effects are reversed by both L-Arg[28] and tetrahydrobiopterin (NOS cofactor);[24] L-Arg also abolishes the associated increase in ROS.[20] NO donor pretreatment has been shown to enhance

Received: January 29, 2013

   dx.doi.org/10.1021/jm400146r | *J. Med. Chem.* XXXX, XXX, XXX−XXX

Table 1. Structures and Associated Codes for Key NOHA and Synthesized Test Compounds

Structure	Code
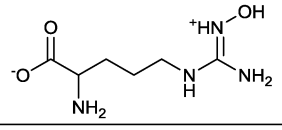	NOHA
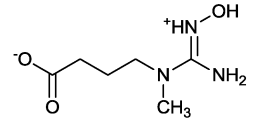	1a
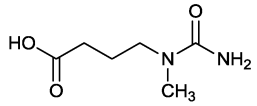	1a(u)
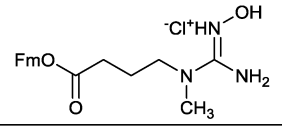	1b
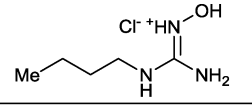	1c
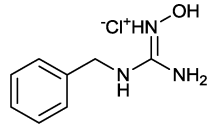	1d
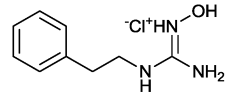	1e
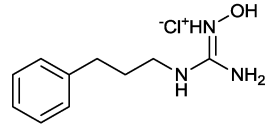	1f
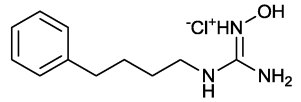	1g
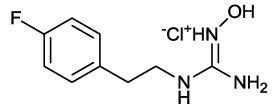	1h
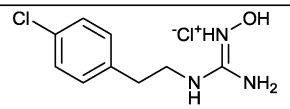	1i
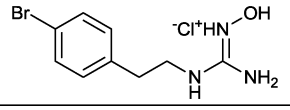	1j

Structure	Code
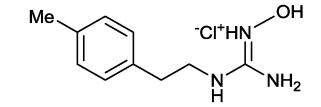	1k
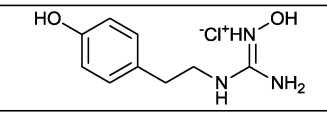	1m
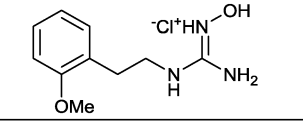	1n
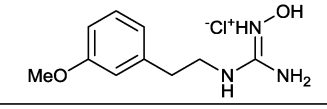	1p
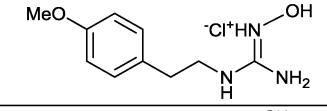	1q
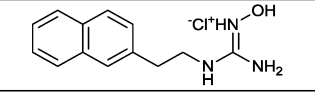	1r
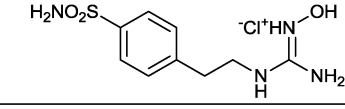	1s
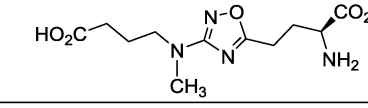	4
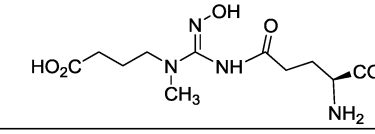	8
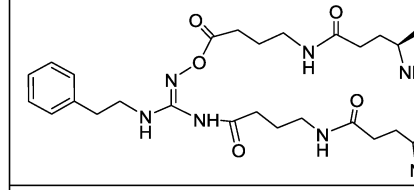	9
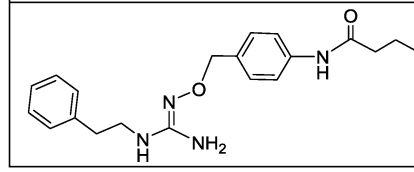	10

renal function in ischemic models[30] and to suppress expression of endothelin-1,[31] a potent vasoconstrictor that is increased in postischemic kidneys.[32] Delivery of exogenous NO may, therefore, offer several levels of protection in ARF.

Progress toward novel NO donor drugs has been disappointingly slow, primarily on account of the difficulty in designing drugs that reproduce the site-specific effects of endogenous NO, which is driven by the highly regulated nature of eNOS and the limited reach of NO from its source of generation.[33] The *N*-hydroxyguanidines (NHGs) include the intermediate in NOS-mediated synthesis of NO, N^{ω}-hydroxy-L-arginine (NOHA), and might offer a fresh approach to tissue-selective NO donor drugs.[34] Some NHGs are known to be metabolized by NOS,[35] as well as a range of other abundant enzymes, such as cytochrome P450s,[36] peroxidases,[37] and XO,[38] offering the potential to generate NO and possibly to reduce enzyme-derived ROS generation,[38] in a nonselective manner throughout the body. NHGs have two accessible functional groups (−OH and $-NH_2$), which allow manipulation into prodrugs through esterification or amidation. With a view to imparting renoselectivity to NHGs, we sought to design, synthesize, and test glutamyl-protected drugs, a strategy

dx.doi.org/10.1021/jm400146r | J. Med. Chem. XXXX, XXX, XXX−XXX

Scheme 1[a]

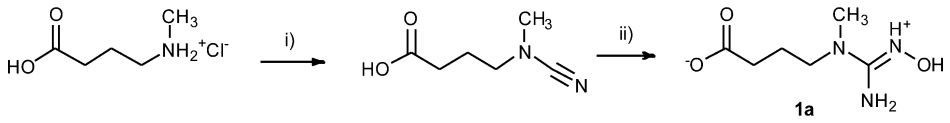

[a]Reagents and conditions: (i) BrCN, NaOAc, MeOH, 0 °C to rt, 2 h; (ii) $NH_2OH{\cdot}HCl$, KOH (cat.), MeOH, reflux, 5 h.

that has previously been employed in protecting the active moiety of L-DOPA for use in ARF.[39−42] This approach exploits the relatively high expression of γ-glutamyl transpeptidase (γ-GT; EC 2.3.2.2) in the kidney (5−10 times higher than in liver or pancreas).[43,44] The enzyme acts to cleave the glutamate adduct, with a view to promoting renoselective activation of the protected compound and avoiding renal "steal" that would accompany nonselective vasodilatation. The ideal glutamyl-protected product, therefore, would be biologically inert, except in the presence of renal tissue, where it would be activated to cause tissue-specific, NO-mediated vasodilatation that was not necessarily dependent on a functional endothelium.

RESULTS

Proof of Principle: Synthesis of Biologically Active Parent and Glutamyl-Protected NHG prototypes. *Prototype NHG Parent Drug and Equivalent Urea (Negative Control).* A prototype parent drug (**1a**; Table 1) was synthesized. **1a** had similarities to NOHA, but without the α-amino group, which was considered to present problems for downstream modification of the molecule in prodrug development; other deviations from NOHA were the addition of an *N*-methyl group and a shorter carbon chain length. Synthesis adopted the common two-step reaction[45−50] involving cyanization of *N*-methyl-4-aminobutanoic acid with cyanogen bromide, followed by nucleophilic addition of hydroxylamine to the resultant cyanamide (Scheme 1). This compound exists as a zwitterion and is soluble in water.

The equivalent urea (**1a**(**u**)) was synthesized via the same intermediate cyanamide but followed by acidic hydrolysis.

[Nitrite + Nitrate] (NO_x) Generation and Vasodilator Activity of NHG Parent Drug Prototypes. The endogenous NHG, NOHA (positive control; 100 μM), was found to generate NO_x (a surrogate marker for NO) in substantial quantities (5−11 μM) after incubation with xanthine (X)/XO, and in rat liver, renal cortex, and renal medullar tissue extracts (1 h, 37 °C). The specific XO inhibitor, allopurinol (100 μM), inhibited X/XO-mediated NO_x generation, while the NOS inhibitor, N^{ω}-nitro-L-arginine methyl ester (L-NAME; 200 μM) abolished the NO_x generation associated with liver extracts and substantially inhibited that in both cortical and medullary renal tissue (Figure 1A). γ-GT did not induce NO_x generation from NOHA (Figure 1A).

Product **1a** (100 μM) was found to have a similar NO_x-generating profile to NOHA in the presence of X/XO, but the NO_x yield in tissue extracts (1−4 μM) was lower than that for NOHA (Figure 1B).

X/XO failed to induce NO_x generation from the urea counterpart (**1a**(**u**)) of **1a**, while low NO_x concentrations (∼1 μM) measured in tissue extracts treated with **1a**(**u**) were not inhibited by L-NAME and were not different from those found in tissue extracts alone (Figure 1C).

To assess the vasodilator properties of product **1a** in comparison to NOHA, precontracted, endothelium-intact rat aortic rings (±L-NAME, 200 μM) were employed. The endothelium-dependent vasodilator, acetylcholine (ACh), was used to test the functional integrity of the endothelium and as an indicator of the effectiveness of NOS inhibition by L-NAME (Figure 2). NOHA (100 μM) was found to be an effective vasodilator that was only partially inhibited by L-NAME. Product **1a** (100 μM), on the other hand, had weak vasodilator properties that were abolished by L-NAME.

Prototype Prodrugs. To impart potential for renoselectivity to **1a**, a γ-glutamyl group was conjugated onto the guanidino *N*-OH to generate a protected molecule with the potential to be a substrate for γ-GT. The glutamate moiety was derived from commercially available difluoren-9-ylmethyl protected glutamic acid (Fmoc-Glu-OFm), the protecting group of which can be removed easily by organic base under mild conditions. To make the side-chain of **1a** match the protecting protocol, the terminal carboxylic group was masked with fluoren-9-ylmethyl before it was reacted with cyanogen bromide and, subsequently, with $NH_2OH{\cdot}HCl$, to generate the NHG, **1b** (Scheme 2).

Reaction of **1b** with Fmoc-Glu-OFm in the presence of *N*-(3-dimethylaminopropyl)-*N*′-ethylcarbodiimide hydrochloride (EDC) initially formed the linear *O*-glutamate **2**, as confirmed by TLC and ^{1}H NMR spectra. However, with time and during work up and purification, it gradually transformed into the heterocyclic derivative **3** with the loss of a molecule of water: fractions collected as the linear product **2** from column chromatography became a mixture of products **2** and **3** after solvent removal. This cyclization process continued during the process of Fm and Fmoc removal under basic conditions and was accompanied by expulsion of pyroglutamic acid and regeneration of the parent NHG (Scheme 3).

An alternative approach was to introduce the glutamyl group into the amino moiety of the parent compound (Scheme 3). Although this is not the site for NO generation from the NHG, it was considered likely that the bulky glutamyl group could sterically hinder enzyme-mediated release of NO. For this purpose, Boc protection was employed because the *N*-OH group is more nucleophilic and reactive than $-NH_2$. This resulted in a stable intermediate **5**, but the same 1,2,4-oxadiazole **3** formed slowly again once the *O*-Boc group was removed in CF_3CO_2H/DCM. The process continued throughout deprotection of Fm/Fmoc in Et_3N/DCM and during workup and purification, although the formation of pyroglutamic acid was found to be much slower in this case because the amide bond is stronger than that of the ester.

Because of this complication, we obtained 1,2,4-oxadiazoles **3** in ∼50% yield and pure **4** (Table 1). The expected product **7** could not be isolated on account of its rapid decomposition; compound **8** (Table 1) was highly hygroscopic and found to readily degrade to **4** as monitored by NMR spectroscopy (Scheme 3).

Bioactivation of Prototype Prodrugs by γ-GT. The cyclic glutamyl-protected adduct of **1a**, compound **4** (100 μM), failed to induce vasodilatation at this concentration, irrespective of preincubation with γ-GT (Figure 3). Prodrug **8** was tested

dx.doi.org/10.1021/jm400146r | J. Med. Chem. XXXX, XXX, XXX−XXX

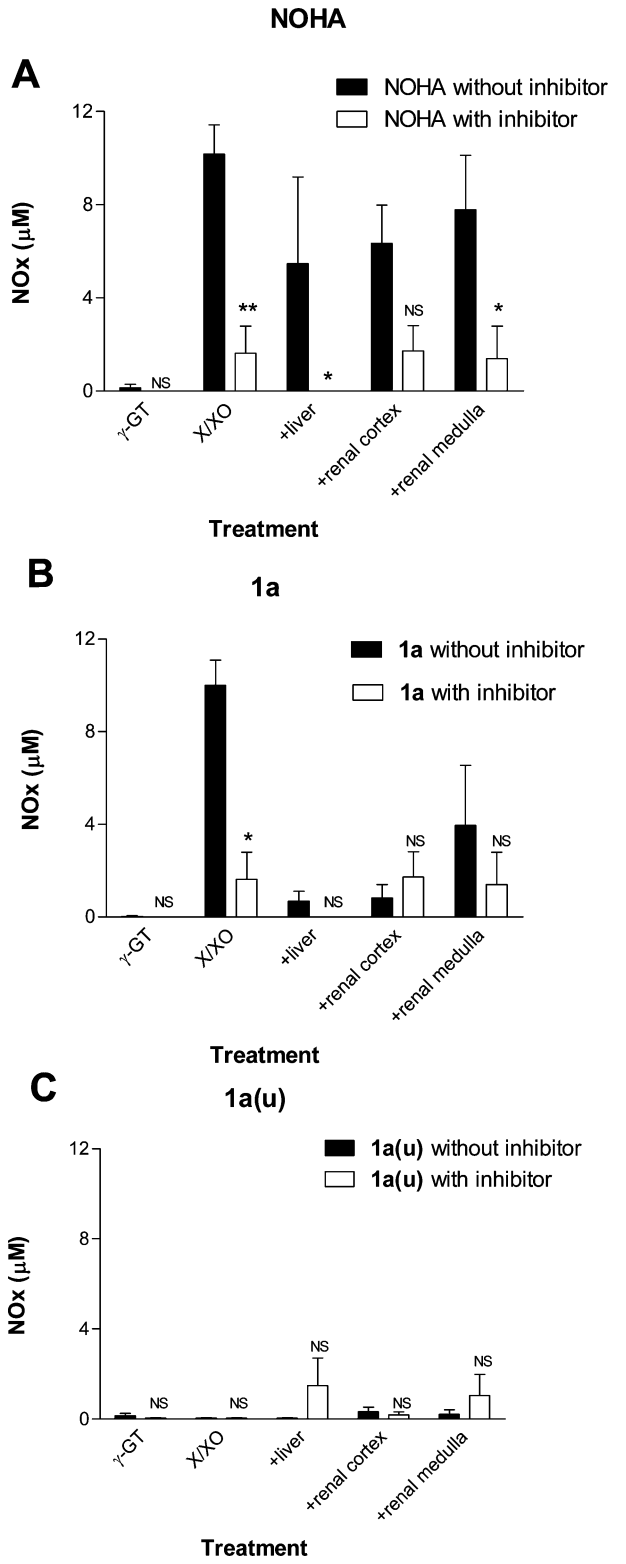

Figure 1. Release of NO_x from (A) the endogenous NHG, NOHA (n = 4–5), (B) the novel NHG, **1a** (n = 4–5), and (C) the corresponding urea **1a**(**u**) (negative control, n = 4–5; all 100 μM) in the presence of γ-GT (100 mU/5 mM gly/gly), xanthine/xanthine oxidase (X/XO; 100 μM/100 mU), and rat tissue homogenates. Parallel experiments were conducted in the presence of specific inhibitors (5-sulfosalicylate (100 μM) for γ-GT, allopurinol (100 μM) for XO, and the NOS inhibitor, L-NAME (200 μM) for the tissue homogenates) to help confirm enzyme specificity. *P < 0.05, **P < 0.01; paired t-test in presence vs absence of specific inhibitor.

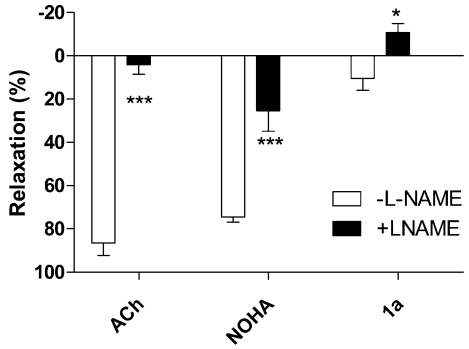

Figure 2. Vasodilator activity of ACh, NOHA and product **1a** in endothelium-intact, precontracted rings of rat aorta in the presence and absence of the NOS inhibitor, L-NAME (200 μM). ACh and product **1a**-mediated vasodilatation was deemed to be almost exclusively NOS-dependent, while that induced by NOHA was considered to be partially NOS-independent. *P < 0.05, ***P < 0.001, paired Student's t-test ± L-NAME.

for vasodilatation and found to be inactive in the absence of γ-GT but produced a modest (~18%) relaxation after preincubation with γ-GT that was abolished by the NO scavenger, oxyhemoglobin (Hb; 10 μM).

Design and Synthesis of Parent NHG Drug Library. On the basis of the preliminary results from the proof of principle study, 15 NHGs were synthesized (Table 1: 12 novel, 3 known **1c–s**) bearing different alkyl and aryl side-chains, following the same two-step procedure[45−50] from commercial or in-house amines,[51] with a view to optimizing NO-donor parent drug efficacy and establishing a structure–activity relationship.

All NHGs have a typical resonance at ca. δ_C 158 ppm for the guanidino carbon in the ^{13}C NMR spectrum. Using DMSO-d_6 as solvent, all ^1H NMR spectra for the N-monosubstituted final products showed four distinctive proton signals for the protonated hydroxyguanidine group (ca. δ_H 7.7 for NH_2, δ_H 8.0 for alkyl or aryl NH, δ_H for N′H, δ_H 10.4 for OH). The assignments were based on integration/coupling pattern (Supporting Information (SI) Figure S1) and 2D ^1H–^{13}C HMBC spectrum (Figure S2) in SI represented by **1g**.

The synthetic NHG yields (Table 2) were affected by repeated recrystallization steps necessary to achieve sufficiently high purity of the product and satisfactory microanalysis results. In the case of **1s**, even repeated recrystallization failed to generate product of sufficient purity. Instead, Boc protection followed by column chromatography and removal of the protecting group by 4N HCl in dioxane was used to generate pure product.

The vasodilator effects of the synthesized compounds were tested in vitro using endothelium-intact rat isolated aortic rings. The principal aim of the screen was to find compounds that were not entirely dependent on NOS for activation but for which the majority of the vasodilator activity was nevertheless dependent on the NO:sGC pathway. Experiments were therefore conducted in the presence of the NOS inhibitor, L-NAME (200 μM), and the reversibility of responses was assessed using the sGC inhibitor, 1H-[1,2,4]oxadiazolo[4,3-a]quinoxalin-1-one (ODQ; 50 μM). Promising compounds were tested further using Hb (10 μM), an acknowledged scavenger of NO, and L-Arg (100 μM; approximate plasma levels), which might compete with the drug under endogenous conditions, not only at the active site for NOS but also at the system y^+/CAT amino acid transporters,[52,53] should NHGs

dx.doi.org/10.1021/jm400146r | J. Med. Chem. XXXX, XXX, XXX–XXX

Scheme 2[a]

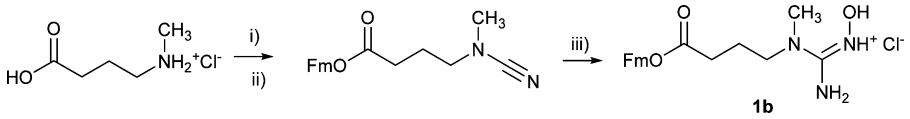

[a]Reagents and conditions: (i) FmOH, TsOH, reflux; (ii) BrCN, NaOAc, MeOH; (iii) $NH_2OH{\cdot}HCl$, K_2CO_3, MeOH.

Scheme 3[a]

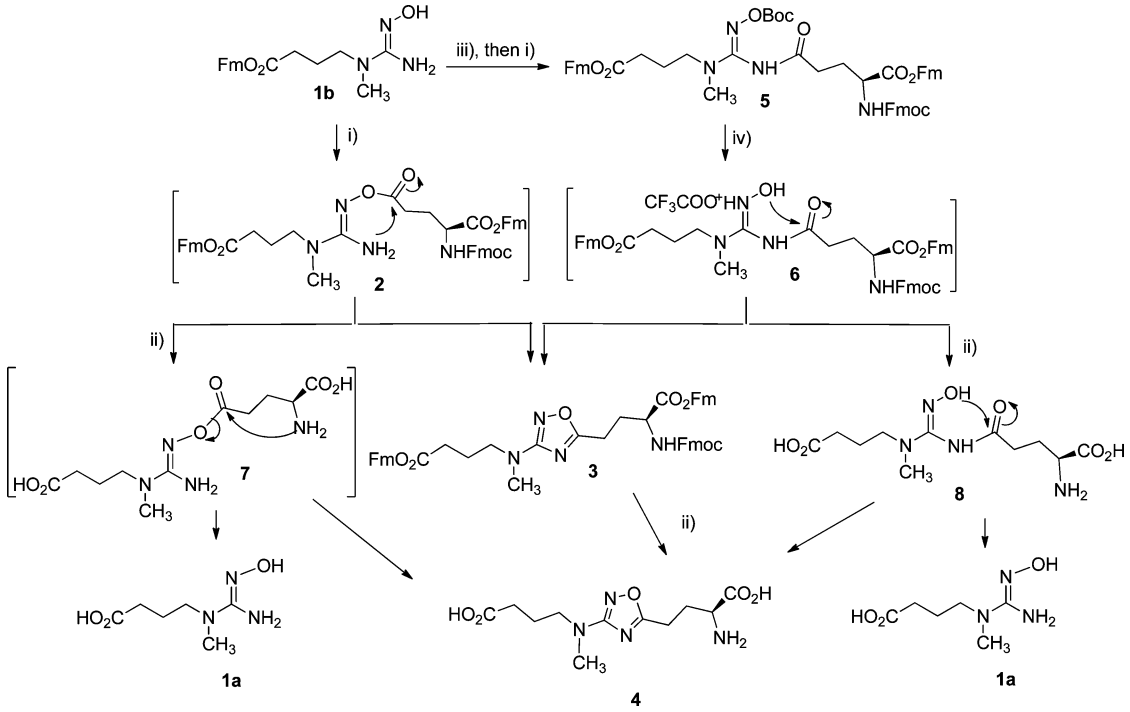

[a]Reagents and conditions: (i) Fmoc-Glu-OFm, HOBt, EDC, DCM, DMF, rt, 3 d; (ii) Et_3N, DCM; (iii) $(Boc)_2O$, DMF, H_2O, K_2CO_3, 0 °C, 2 h, 100%; (iv) CF_3COOH, DCM, 0 to rt, 2 h.

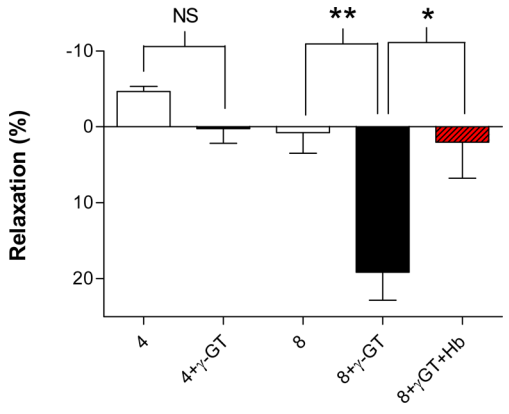

Figure 3. Vasodilator activity of two prototype prodrugs (**4**, **8**) with and without preincubation with γ-GT. Prodrug **4** failed to cause vasodilatation, irrespective of the presence of γ-GT. However, prodrug **8** was induced to cause modest vasodilatation after incubation with γ-GT (100 mU/mL, 60 min, 37 °C), and the effect was abolished by the NO scavenger, Hb (10 μM). *$P < 0.05$, **$P < 0.01$ (Dunnet's post-test following one-way ANOVA for product **8** ± γ-GT and ± [γ-GT + Hb]; $n = 5–9$). NS: no statistical difference between response to **4** ± γ-GT ($n = 5$; paired Student's t test).

utilize these transporters to access cells. Parallel experiments in the absence of L-NAME confirmed the extent of the contribution of NOS to vasodilatation. The conventional endothelium-dependent vasodilator, ACh, was used to both confirm the function of the endothelium in test rings and to validate the model with respect to the inhibitors used (Figure 4A). The results are summarized in Table 2 and shown in their entirety for selected test compounds in Figure 4B,C.

The results revealed that drug efficacy was improved by substitution of the terminal carboxylic acid moiety of product **1a** with a methyl group (**1c**) or an aromatic ring (**1e**) and that the length of the carbon chain backbone of the molecule (**1d–g**) also affected efficacy, with a chain length of 2C (**1e**) appearing optimal for both vasodilator activity and dependence on sGC. Substitution on the aromatic ring with F (**1h**), Cl (**1i**), or Br (**1j**) reduced the potency of the NHG with respect to vasodilatation and also reduced the dependence on sGC. A similar effect was seen with $-CH_3$ substitution (**1k**) at this position and, while −OH (**1m**) substitution apparently increased vasodilator activity, there was a concomitant loss in sGC-dependence. Substitution with a methoxy group at three different positions on the aromatic ring (**1n–q**) had a detrimental effect in terms of dependence on sGC. Substitution with $-SO_2NH_2$ (**1s**) at the same position abolished the vasodilator effects of the compound. Finally, addition of a second aromatic ring (**1r**) also reduced efficacy.

Figure 4 illustrates the extended testing that was conducted on **1e** as the lead parent drug identified from the screen; the

dx.doi.org/10.1021/jm400146r | J. Med. Chem. XXXX, XXX, XXX–XXX

Table 2. NHG Parent Compound Synthetic Yield and Bioactivity in Rat Aortic Rings (Shaded Box Indicates Lead Selection)

Code	Yield (%)	Log EC_{50} (M)	ODQ Reversal (%)
1a	45	N/A – preliminary tests only	N/A – preliminary tests only
1a(u)	N/A	No Effect	N/A
1c	76	-4.5 ± 0.2	100±1
1d	45	-4.9 ± 0.4	37 ± 10
1e	70	**-4.6 ± 0.1**	**75 ± 16**
1f	58	-4.8 ± 0.1	68 ± 12
1g	55	-3.2 ± 1.6	28 ± 12
1h	46	-4.2 ± 0.5	11 ± 15
1i	44	-4.0 ± 0.1	11± 14
1j	67	-4.8 ± 0.1	34 ± 14
1k	30	-4.9 ± 0.2	35 ± 14
1m	40	-4.2 ± 0.4	N/A
1n	46	-4.7 ± 0.1	14 ± 18
1p	53	-5.4 ± 0.2	9 ± 2
1q	58	-4.3 ± 0.1	40 ± 4
1r	79	-4.3 ± 0.6	1 ± 8

endothelium-dependent vasodilator, ACh, and NOHA were tested in parallel for reference purposes. ACh-mediated vasodilatation in precontracted, endothelium-intact rat aortic rings was abolished by L-NAME, Hb, and ODQ. However, L-Arg did not significantly affect the vasodilator properties of ACh (Figure 4A). Treatment of aortic rings with NOHA induced concentration-dependent vasodilatation that was abolished by ODQ and substantially inhibited by both L-NAME and Hb (Figure 4B). The effect was also inhibited by coincubation with L-Arg. Product **1e** had weaker vasodilator activity than NOHA in the absence of the NO:sGC pathway inhibitors and L-Arg, while its effects were all but abolished by ODQ. However, the inhibitory effects of L-NAME and Hb were substantially weaker than they were for NOHA, while responses to product **1e** were slightly augmented by L-Arg. The crystal structure of the chosen lead parent drug, **1e**, is shown in Figure 5.

Design and Synthesis of NHG Prodrug, Based on Parent Lead. Having selected product **1e** as the lead parent drug, experimental procedures were initiated to synthesize a range of glutamyl protected prodrugs. The task was colored by the issues of cyclization that had come to light in the proof of principle phase of the study. It was deduced that the reasons for cyclization were 2-fold (Scheme 3): the *N*-OH or $-NH_2$ groups are ideally positioned with respect to the γ-glutamyl for generation of a highly stable five-membered aromatic ring and the tendency for the formation of pyroglutamic acid due to the instability of the *N*-hydroxyguanido ester/amide. A detailed description of a range of strategies used to disrupt the potential for cyclization and the evolution of the prodrugs has been reported elsewhere.[54]

Dipeptidyl Protected NHG Prodrug. A dipeptidyl prodrug *O*,*N*-bis(GABAGlu)-NHG (prodrug **9**; Table 1) was successfully synthesized using two equivalents of dipeptide to protect both the *N*-OH and the $-NH_2$ groups of the NHG[54] in order to deprive these groups of the opportunity to attack the nearby C═O group, causing cyclization (Scheme 4). A γ-aminobutyric acid (GABA) fragment[55] was employed as a simplified version of Glu, which as evidenced above, has a strong suicidal tendency through formation of lactam. The glutamyl residue itself serves as the recognizable residue for γ-GT activity. The amidic bond between the two amino acids was considered to be as stable as a normal peptide bond and able to survive the workup. Upon incubation with γ-GT, it was envisaged that the enzyme would cleave the terminal glutamyl group; the newly exposed linkers on both the *O* and *N* limbs

dx.doi.org/10.1021/jm400146r | J. Med. Chem. XXXX, XXX, XXX−XXX

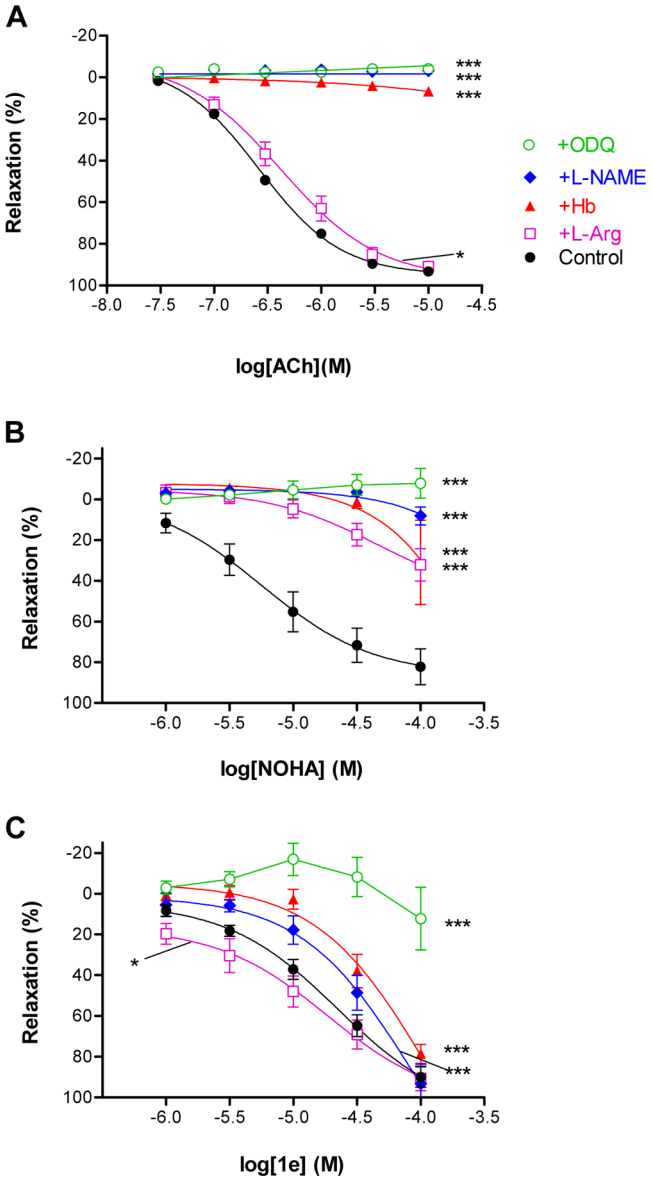

Figure 4. Log concentration−response curves for (A) ACh, (B) NOHA, and (C) product **1e** in the absence (control) and presence of the NOS inhibitor, L-NAME (200 μM), the endogenous substrate for NOS, L-Arg, the NO scavenger, Hb (10 μM), and the sGC inhibitor, ODQ (50 μM). *P < 0.05, ***P < 0.001, 2-way ANOVA with Bonferroni post-test (n = 12−15 for ACh; n = 4−9 for NOHA and n = 6−8 for **1e**).

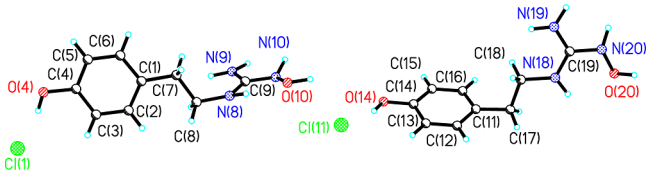

Figure 5. X-ray structure of product **1e**, the lead parent drug chosen for prodrug development.

would spontaneously drop off as an effect of thermodynamically favored cyclization, releasing the parent NHG in the process.

However, prodrug **9** failed to induce relaxation, irrespective of preincubation with γ-GT (data not shown).

NHG Prodrugs with an Aromatic Linkage. The inability of γ-GT to activate the GABA-linked prodrug (**9**) prompted the application of another self-immolative spacer, the aminobenzyl ether (compound **10** in Scheme 5; Table 1). γ-Glutamyl anilines, especially p-nitro glutamylanilide, are well-known substrates for γ-GT.[56−58] Prodrugs bearing a glutamylaniline moiety would be more likely to represent suitable substrates for γ-GT. In addition, similar linkage has been employed previously in anticancer prodrugs design.[59−69]

Prodrug **10** was successfully synthesized from p-glutamylaminobenzyloxyamine and amino(phenethyliminio)-methanesulfonate in modest yield after removal of the protecting group. Details of the synthetic procedure for **10** are published elsewhere.[54] Prodrug **10** induced modest relaxation of rat aortic rings that was enhanced after incubation with γ-GT (Figure 6A). Responses in both the presence and absence of γ-GT showed substantial reversal upon addition of ODQ.

On the back of these findings, the vasodilator activity of prodrug **10** was tested in the isolated perfused rat kidney, alongside the parent compound, **1e**; prodrug **9** was included as a negative control on the basis that it did not induce relaxation in rat aortic rings, irrespective of the presence of γ-GT. In keeping with the findings in aortic rings, prodrug **9** failed to induce vasodilatation in isolated perfused kidneys, even at concentrations as high as 250 μM (Figure 6B). Prodrug **10**, on the other hand, induced concentration-dependent vasodilatation in the kidney (EC_{50} ~50 μM). Renal metabolism profiles for prodrug **10** in rat kidney homogenates illustrate that compound **1e** is generated from prodrug **10** in a time and concentration-dependent manner over a 45 min incubation period (Figure 6C).

DISCUSSION AND CONCLUSIONS

This research program adopted a multidisciplinary approach to first prove principle and then design and screen for a glutamyl-protected NHG prodrug that might ultimately offer renoselectivity for use in ARF. Prototype parent and prodrugs successfully proved principle, but also highlighted a propensity for cyclization of simple glutamyl-protected NHG prodrugs, which prevented effective cleavage by γ-GT. A library of parent molecules was subsequently designed and screened for NO:sGC-mediated vasodilator effects and a lead compound selected for glutamyl protection. The cyclization problem was overcome by incorporation of an aromatic linker between the glutamyl and NHG moieties, which was spontaneously lost after γ-GT-mediated cleavage of the glutamyl group. Using this technique, a suitable prodrug (**10**) was synthesized and tested in several models to confirm sensitivity to γ-GT-mediated activation, decomposition to the parent drug in the presence of rat renal tissue and vasodilator activity in isolated rat perfused kidneys. The results confirm that glutamyl-mediated protection of NHGs represents a valid approach to NO-induced, renoactive vasodilatation that could have therapeutic advantages in areas of unmet clinical need, and ARF in particular.

The proof of principle study confirmed that activity of the parent drug required the guanidino moiety (the corresponding urea was inactive) and was induced by X/XO enzyme preparations and NOS in tissue extracts. In addition, it was established that it is possible to generate γ-GT-dependent NHG-derived prodrugs, providing the molecule does not cyclize. The modest vasodilatory efficacy of both the parent molecule and the prodrug indicated that there was substantial

dx.doi.org/10.1021/jm400146r | J. Med. Chem. XXXX, XXX, XXX−XXX

Scheme 4. Design of *O,N*-Bis(GAbAGlu)-NHG Prodrug

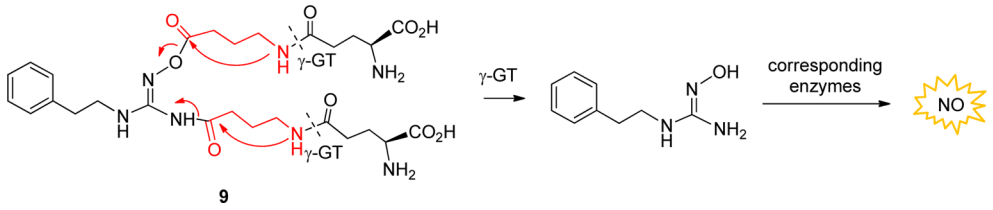

Scheme 5. Design of a γ-Glutamyl Prodrug of NHG with an Aromatic Linker

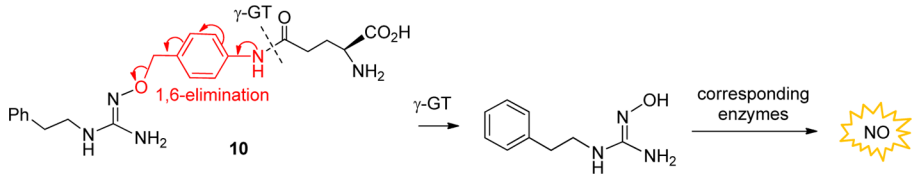

room for improvement in terms of optimization of chemical structure. While prodrug **8** confirmed that the concept of glutamyl protection was valid, the propensity toward cyclization of this product also served notice that optimization of the structure was necessary and that a more sophisticated approach would be required to develop stable prodrugs that would resist cyclization and retain the potential for γ-GT-mediated activation. Similarly, there was room to optimize the parent drug to generate more NO and to be less NOS-dependent in case NOS was dysfunctional in the target disease state.

NOHA, and a growing literature relating to synthetic NHG generation,[34,70−72] provided the basis for design and synthesis of novel NHGs that might have improved pharmacological profiles. The principal difference between the prototype developed for the proof of principle study (product **1a**) and NOHA was the absence of the α-amino group, which was deemed necessary to increase hydrophobicity and to avoid protection/deprotection issues that were likely to arise at the conjugation stage of prodrug design. However, this molecule was found to only have weak NO_x-generating capabilities and vasodilator properties compared to the endogenous NHG, NOHA. The first step in the evolution of the molecule was to render it less polar by replacement of the terminal carboxylic group with first, a methyl group (product **1c**), and then an aromatic ring (products **1d−s**). In addition, the methyl group on the central N was considered redundant and was removed. Together, these modifications markedly increased the vasodilatory effect of the compounds in comparison to the prototype **1a**. Subsequent modifications to the structure revealed that the optimal chain length for the carbon backbone was ∼2C (**1e**); increasing or decreasing the carbon chain length reduced the dependence of the response on sGC. A similar structure−activity relationship had previously been shown for analogues of NOHA.[73] Finally, it was established that substitution on the aromatic ring invariably reduced drug efficacy and/or dependence on sGC. Of the conformations investigated, the desirable molecular characteristics to confer vasodilator effects that were predominantly (>75%) mediated by stimulation of sGC were a nonpolar aromatic terminal group linked to the guanidino moiety by a short carbon chain (2C). The lead compound from this screen was therefore deemed to be product **1e**, and we undertook to explore the vasodilator characteristics of this particular parent drug in detail.

To fully appreciate the results obtained with **1e**, it is important to first consider those obtained with NOHA, the actions of which were found to be almost entirely dependent on NOS activation, NO generation, and stimulation of smooth muscle sGC. Interestingly, however, the vasodilator activity of NOHA was inhibited by L-Arg, suggesting that L-Arg effectively competes with NOHA at the active site of eNOS and/or at the amino acid transporter system y^+.[52,74] The polar characteristics of NOHA suggest that it is unlikely to be able to cross the lipid bilayer and its structural similarity to L-Arg could allow it to hijack the amino acid transporter systems. It is also apparent that, while the vasodilator properties of NOHA are dependent on NOS, they do not require the enzyme to be Ca^{2+}-activated (e.g., by ACh, shear stress, hypoxia).

In stark contrast to NOHA, **1e** was considerably less sensitive to L-NAME and Hb-mediated inhibition while retaining almost exclusive reliance on sGC activation. These results imply that not only is the activation of this drug largely independent of NOS but that the NO generated to stimulate sGC is released at a site relatively inaccessible to Hb and in close proximity of sGC (i.e., inside smooth muscle cells, as opposed to endothelium). Crucially, the effects of product **1e** were not inhibited, but were perhaps even enhanced, by L-Arg. We argue that the increased hydrophobicity of **1e** enables it to bypass the amino acid transporter systems, eliminating the risk of L-Arg-mediated inhibition in vivo, a distinct advantage over NOHA for in vivo activity in the face of abundant L-Arg.

Effective prodrug design proved challenging. It was obvious from the outset that, while generation of glutamyl adducts undoubtedly protected the resultant molecule from tissue-mediated NO generation, retaining characteristics necessary for γ-GT-mediated activation was complicated by the propensity of the products to spontaneously cyclize. It was very difficult to isolate pure prototype prodrug **8** because it spontaneously transformed into **4**. The solution to the problem came in the form of an aromatic linker[54] that both prevented cyclization and spontaneously dropped out of the molecule after cleavage of the glutamyl group by γ-GT. The resulting compound (prodrug **10**) had weak vasodilator properties in rat aortic rings that were significantly enhanced by addition of γ-GT and were mainly sGC-dependent. Release of the corresponding parent drug (**1e**) was confirmed in rat kidney extracts, and prodrug **10** was found to have vasodilator effects in rat isolated perfused kidneys that were not evident for a GABA-linked equivalent (prodrug **9**).

In summary, we have successfully developed a novel reno-active NO donor prodrug **10**. The key features of the molecule

dx.doi.org/10.1021/jm400146r | J. Med. Chem. XXXX, XXX, XXX−XXX

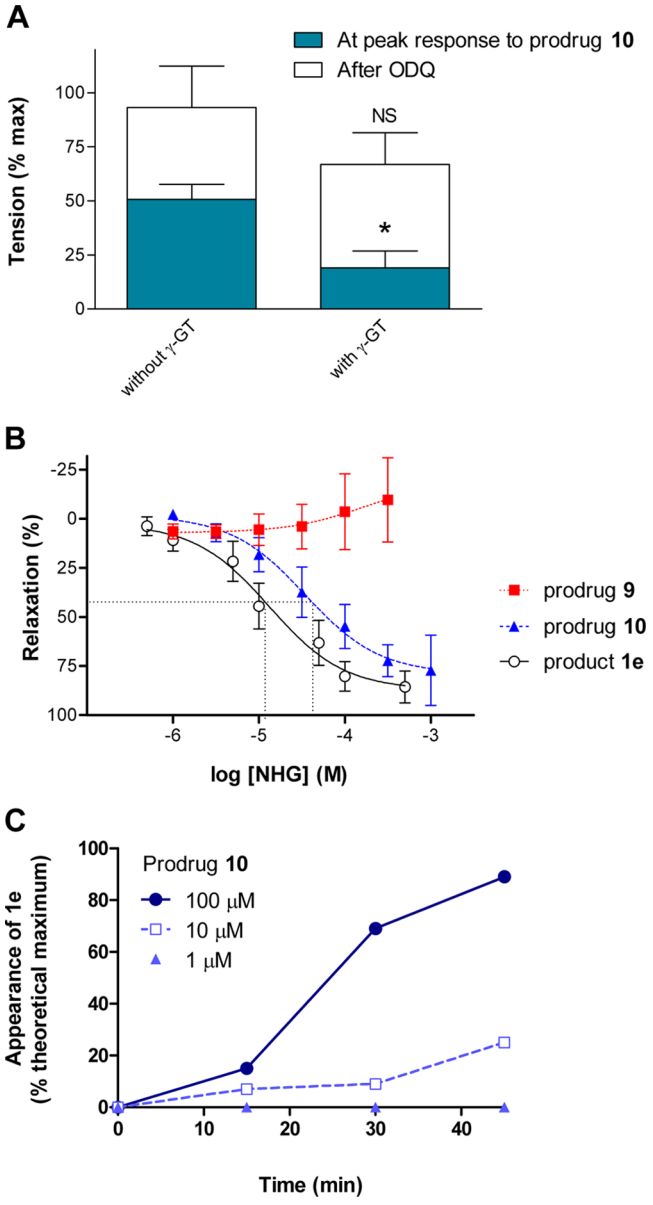

Figure 6. (A) Effect of preincubation of prodrug **10** (100 μM) with γ-GT (100 mU/mL) on vasodilator responses in precontracted rat aortic rings in the presence and absence of the sGC inhibitor, ODQ (50 μM). NS: no significant difference, *$P < 0.05$, paired Student's t-test vs response in absence of γ-GT; $n = 5$. (B) Vasodilator effect of the lead prodrug **10**, its parent counterpart, **1e**, and a glutamyl-protected NHG that is not a substrate for γ-GT (prodrug **9**; negative control) in the isolated perfused rat kidney model. (C) Appearance of parent compound **1e** in rat kidney homogenates treated with prodrug **10** (1, 10, 100 μM) with time.

are afforded by the nonselective NO-generating properties of the parent molecule, coupled with the protective effects prescribed by the glutamyl adduct. Its vasodilator properties are enhanced by the enzyme γ-GT, which is most highly expressed in the renal medulla and, unlike the enzyme-resistant prodrug **9**, it successfully induces vasodilation in isolated perfused kidneys. The specific enzyme(s) involved in the activation of the cleaved parent NHG in renal tissue is not yet known, but the literature would suggest that a range of enzymes with peroxidase activity could effect the activation step, generating NO or possibly HNO that would rapidly isomerize to NO at physiological pH.

While we acknowledge that prodrug **10** does not possess perfect characteristics for renoselectivity, its properties certainly indicate that glutamyl protection of NHGs is a valid approach to development of a new generation of drugs for use in ARF, the primary target of unmet need, but also potentially in other renal conditions that might benefit from increased renal blood flow, including hypertension. Further research with prodrug **10** is merited in animal models of cross-clamping and sepsis to test the viability of this approach in clinically relevant applications. In vivo experiments would test whether the activity seen in rat isolated kidneys translates into true renoselectivity, as defined by increased blood flow without an impact on systemic blood pressure and would identify optimal concentrations required to prevent ARF. While the acute nature of the primary disease target ensures that toxicity on account of chronic dosing is not a consideration, acute toxicity of NHGs in this clinical setting is not known. An issue that would require special attention in this regard is the potential for enhanced generation of $ONOO^-$ in disease states.

This study represents a significant step forward in the quest for an effective preventative agent for use in ARF to address an urgent clinical need. The results point to successful development of a prodrug that is active in renal tissue and has the potential for renoselectivity. Optimization of the prototype and testing in models of ARF are merited.

EXPERIMENTAL SECTION

NMR spectra were recorded on a Bruker Advance 300 (^{1}H 300 MHz, ^{13}C 75.4 MHz) or 400 (^{1}H 400 MHz, ^{13}C 100.6 MHz) spectrometer. Chemical shifts (δ) in ppm are given relative to Me_4Si, coupling constants (J) are given in Hz. Low resolution and high resolution electrospray mass spectra were recorded on a Micromass LC-T (time-of-flight). Analytical TLC was carried out on either Merck Silica 60 F_{254} or RP-18 F_{254S} plates. Purity of the tested compounds was >95% based on either elemental analysis or HPLC analysis.

General Procedure for the Synthesis of NHGs. A 3 M solution of cyanogen bromide in DCM (1 equiv) was added dropwise to an ice-cooled suspension of the amine or corresponding salt (commercially available or in house-made) and sodium acetate (3 equiv) in MeOH with stirring. The mixture was stirred in an ice bath for 2 h, and then the ice bath was removed and the reaction mixture was allowed to stir at room temperature overnight. After removal of the solvent in vacuum, the residue was partitioned between DCM and water. The aqueous layer was extracted with DCM three times. The combined organic phases were dried over $MgSO_4$. Removal of the solvent under reduced pressure and purification using column chromatography (silica gel, Pet ether/Et_2O 1:2) gave the intermediate cyanamide. The cyanamide was mixed with hydroxylamine hydrochloride (1 equiv) and potassium carbonate (0.1 equiv) in anhydrous MeOH. The mixture was heated at reflux for 6 h under an argon atmosphere. After cooling, the solvent was removed at reduced pressure and the desired product was crystallized from CH_2Cl_2 and diethyl ether. Further purification was achieved by redissolving the crude product in minimum amount of methanol followed by filtration to remove any insoluble material. Titration of the filtrate with diethyl ether usually led to the precipitation of pure product; if microanalysis was not satisfactory, repeated recrystallization from MeOH/Et_2O was performed.

N-3-Carboxypropyl-N-methyl-N′-hydroxyguanidine ***1a.*** Colorless solid (70%). Found: C, 40.96; H, 7.61; N, 23.76%. $C_6H_{13}N_3O_3$ requires C, 41.14; H, 7.48; N, 23.99%. δ_H (300 MHz, D_2O) 1.79 (quintet, 2H, J 7.2 Hz, CH_2-2), 2.12 (t, 2H, J 7.2 Hz, CH_2-3), 2.91(s, 3H, $NC\underline{H}_3$), 3.26 (t, 2H, J 7.3 Hz, CH_2-1). δ_C (75.46 MHz, D_2O)

dx.doi.org/10.1021/jm400146r | J. Med. Chem. XXXX, XXX, XXX−XXX

23.2, 33.7, 35.7, 50.1, 158.9 (C=NOH), 182.2. *m/z* (ESI^+) 176 $[M + H]^+$, 198 $[M + Na]^+$, 214 $[M + K]^+$.

N-3-Carboxypropyl-N-methylurea ***1a(u)***. *N*-3-Carboxypropyl-*N*-methylcyanamide (284 mg, 2 mmol) was dissolved in 4N HCl solution. The mixture was heated at reflux for 6 h, cooled to room temperature, and extracted with DCM (three times). The combined extracts were dried ($MgSO_4$) and solvent removed under reduced pressure to give a gum-like residue. The residue was purified by column chromatography (silica gel, EtOAc:DCM 6:1) to give the product as a white solid (256 mg, 80%). Found: C, 44.87; H, 7.38; N, 17.54%. $C_6H_{12}N_2O_3$ requires C, 44.99; H, 7.55; N, 17.49%. δ_H (300 MHz, D_2O) 1.57 (quintet, 2H, *J* 7.2 Hz, CH_2-2), 2.11 (t, 2H, *J* 7.2 Hz, CH_2-3), 2.60 (s, 3H, CH_3), 3.01 (t, 2H, *J* 7.2 Hz, CH_2-1). δ_C (75.46 MHz, D_2O) 22.7, 31.4, 34.5, 47.9, 161.4, 178.4. *m/z* (ESI^+) 161 $[M + H]^+$, 183 $[M + Na^+]$.

N-n-Butyl-N′-hydroxyguanidine ***1c***.[49] Colorless crystal (48%). Found: C, 36.09; H, 8.89; N, 25.34%. $C_6H_{14}ClN_3O_3$ requires C, 35.82; H, 8.42; N, 25.07%. δ_H (300 MHz, DMSO-d_6) 0.86 (t, 3H, *J* 7.4 Hz, CH_3), 1.26 (hexatet, 2H, *J* 7.4 Hz, CH_2-3), 1.48−1.39 (m, 2H, CH_2-2), 3.13 (dt, 2H, *J* 5.8, 7.4 Hz, CH_2-1), 7.68 (br s, 2H, NH_2), 7.96 (t, 1H, *J* 5.8 Hz, NH), 9.82 (br s, 1H, NH), 10.43 (br s, OH). δ_C (75.46 MHz, DMSO-d_6) 158.7, 40.7, 30.9, 19.6, 13.9. *m/z* (ESI^+) 132 $[M-Cl^-]$.

N-Benzyl-N′-hydroxyguanidine Hydrochloride ***1d***.[34] Colorless solid (45%). Found: C, 47.50; H, 5.85; N, 20.97%. $C_8H_{12}ClN_3O$ requires C, 47.65; H, 6.00; N, 20.84%. δ_H (300 MHz, DMSO-d_6) 4.42 (2H, d, *J* 6.4 Hz, CH_2-1), 7.25−7.41 (5H, m, Ar−H), 7.81 (2H, br s, NH_2), 8.40 (1H, t, *J* 6.8 Hz, NH), 9.88 (1H, br s, NH), 10.57 (1H, br s, OH). δ_C (75.46 MHz, DMSO-d_6) 43.5, 127.1, 127.4, 128.4, 137.3, 158.3 (C=NOH); *m/z* (ESI^+) 166 $[M + H]^+$.

N-(4-Phenylethyl)-N′-hydroxyguanidine Hydrochloride ***1e***.[34] Colorless flake crystals (70%). Found: C, 50.12; H, 6.08; N, 19.48%. $C_9H_{14}ClN_3O$ requires C, 50.12; H, 6.38; N, 19.71%. δ_H (300 MHz, DMSO-d_6) 2.79 (2H, t, *J* 7.2 Hz, CH_2-2), 3.43−3.67 (2H, m, CH_2-1) 7.18−7.24 (3H, m, H-2′, 4′, 6′), 7.27−7.32 (2H, m, H-3′, 5′), 7.75 (2H, br s, NH_2), 8.00 (1H, t, *J* 6.4 Hz, NH), 9.88 (1H, br s, N′H), 10.53 (1H, br s, OH). δ_C (75.46 MHz, DMSO-d_6) 34.5, 42.5, 127.2, 129.1, 129.3, 138.6, 159.0 (C=NOH). *m/z* (ESI^+) 180 $[M + H]^+$.

N-(3-Phenylpropyl)-N′-hydroxyguanidine Hydrochloride ***1f***. Colorless flake crystals (58%). Found: C, 52.01; H, 6.90; N, 18.41%. $C_{10}H_{16}ClN_3O$ requires C, 52.29; H, 7.02; N, 18.29%. δ_H (300 MHz, DMSO-d_6) 1.77 (2H, q, *J* 7.2 Hz, CH_2-2), 2.59 (2H, t, *J* 7.2 Hz, CH_2-3), 3.15 (2H, q, *J* 7.2 Hz, CH_2-1), 7.14−7.23 (3H, m, H-2′, 4′, 6′), 7.25−7.31 (2H, m, H-3′, 5′), 7.71 (2H, br s, NH_2), 8.05 (1H, t, *J* 7.2 Hz, NH), 9.82 (1H, br s, NH), 10.43 (1H, br s, OH). δ_C (75.46 MHz, D_2O) 29.4, 31.9, 40.4, 126.2, 128.5, 128.7, 141.5, 158.6 (C=NOH). *m/z* (ESI^+), 194 $[M + H^+]$.

N-(4-Phenylbutyl)-N′-hydroxyguanidine Hydrochloride ***1g***. Colorless flake crystals (55%). Found: C, 53.77; H, 7.82; N, 17.18%. $C_{11}H_{18}ClN_3O$ requires C, 54.21; H, 7.40; N, 17.24%. δ_H (300 MHz, DMSO-d_6) 1.42−1.64 (4H, m, CH_2-2,3), 2.58 (2H, t, *J* 7.2 Hz, CH_2-4) 3.16 (2H, dt *J* 7.2 Hz, *J* 6.5 Hz, CH_2-1), 7.14−7.21 (3H, m, H-2′, 4′, 6′), 7.24−7.29 (2H, m, 3′, 5′), 7.66 (2H, br s, NH_2), 7.92 (1H, t, *J* 6.5 Hz, NH), 9.76 (1H, br s, NH), 10.34 (1H, br s, OH). δ_C (75.46 MHz, DMSO-d_6) 27.9, 28.1, 34.6, 38.6, 125.7, 128.3, 141.9, 158.2 (C=NOH). *m/z* (ESI^+) 208 $[M + H]^+$.

N-2-(4′-Fluorophenyl)ethyl-N′-hydroxyguanidine Hydrochloride ***1h***. Colorless solid (42%). Found: C, 45.93; H, 5.59; N, 18.28%. $C_9H_{13}ClFN_3O$ requires C, 46.26; H, 5.61; N, 17.98%. δ_H (300 MHz, DMSO-d_6) 2.77 (2H, t, *J* 7.1 Hz, CH_2-2), 3.36 (2H, quartet, *J* 7.1 Hz, CH_2-1), 7.07−7.16 (2H, m, H-2′, 6′), 7.26−7.35 (2H, m, H-3′, 5′), 7.72 (2H, br s, NH_2), 7.95 (1H, br t, *J* 5.9 Hz, NH), 9.85(1H, br s, NH), 10.44 (br s, 1H, OH). δ_C (75.46 MHz, DMSO-d_6) 34.0, 42.4, 115.4 (d, $^2J_{CF}$ 20.9 Hz, C-3′, 5′), 131.1 (d, $^3J_{CF}$ 8.1 Hz, C-2′, 6′), 134.8 (d, $^4J_{CF}$ *J* 2.9 Hz, C-1′), 158.5 (C=NOH), 161.5 (d, $^1J_{CF}$ 242 Hz, C-4′). δ_F 117.2; *m/z* (ESI^+) 198 $[M + H]^+$.

N-2-(4′-Chlorophenyl)ethyl-N′-hydroxyguanidine Hydrochloride ***1i***. Colorless solid (46%). Found: C, 42.42; H, 5.08; N, 16.74%. $C_9H_{13}Cl_2N_3O{\cdot}0.2H_2O$ requires C, 42.60; H, 5.32; N, 16.56%. δ_H (300 MHz, DMSO-d_6) 2.79 (2H, t, *J* 7.2 Hz, CH_2-2), 3.38 (2H, quartet, *J* 7.2 Hz, CH_2-1), 7.31 (2H, m, *J* 8.4 Hz, H-2′, 6′), 7.36 (2H, d, *J* 8.4 Hz, H-3′, 5′), 7.72 (2H, br s, NH_2), 7.95 (1H, br t, *J* 5.3 Hz, NH), 9.85 (1H, br s, NH), 10.44 (br s, 1H, OH). δ_C (75.46 MHz, DMSO-d_6) 33.8, 41.7, 128.2, 130.8, 131.0, 137.33, 158.1 (C=NOH). *m/z* (ESI^+) 214 $[M + H]^+$.

N-2-(4′-Bromophenyl)ethyl-N′-hydroxyguanidine Hydrochloride ***1j***. Colorless solid (67%). Found: C, 36.78; H, 4.16; N, 14.28%. $C_9H_{13}BrClN_3O$ requires C, 36.70; H, 4.45; N, 14.26%. δ_H (300 MHz, DMSO-d_6) 2.77 (2H, t, *J* 7.2 Hz, CH_2-2), 3.35−3.43 (2H, m, CH_2-1), 7.22−7.27 (2H, m, H-2′, 6′), 7.47−7.52 (2H, m, H-3′,5′), 7.70 (2H, br s, NH_2), 7.91 (1H, t, *J* 6.3 Hz, NH), 9.81 (1H, br s, NH), 10.42 (1H, br s, OH). δ_C (75.46 MHz, DMSO-d_6) 33.8, 41.6, 119.5, 131.1, 137.7, 158.1 (C=NOH). *m/z* (ESI^+) 260 $[M + H]^+$.

N-2-(4′-Methylphenyl)ethyl-N′-hydroxyguanidine Hydrochloride ***1k***. Colorless solid (30%). Found: C, 52.46; H, 6.94; N, 18.45%. $C_{10}H_{16}ClN_3O$ requires C, 52.29; H, 7.02; N, 18.29%. δ_H (400 MHz, DMSO-d_6) 2.26 (3H, s, CH_3), 2.74 (2H, t, *J* 7.2 Hz, CH_2-2), 7.13 (4H, 2 × d, *J* 8.4 Hz, Ar−H), 7.69 (2H, br s, NH_2), 7.89 (1H, t, *J* 6.5 Hz, NH), 9.82 (1H, br s, NH), 10.36 (1H, br s, OH). δ_C (100 MHz, DMSO-d_6) 21.1, 34.5, 42.5, 129.2, 129.4, 135.6, 135.8, 158.6 (C=NOH). *m/z* (ESI^+) 194 $[M + H]^+$.

N-2-(4′-Hydroxyphenyl)ethyl-N′-hydroxyguanidine Hydrochloride ***1m***. Colorless solid (40%). Found: C, 46.49; H, 5.94; N, 18.05%. $C_9H_{14}ClN_3O_2$ requires C, 46.66; H, 6.09; N, 18.14%. δ_H (300 MHz, DMSO-d_6) 2.67 (2H, t, *J* 7.2 Hz, CH_2-2), 3.26−3.73 (2H, m, CH_2-1), 6.66−6.73 (2H, m, H-3′, 5′), 7.01−7.08 (2H, m, H-2′,6′), 7.65 (2H, br s, NH_2), 7.81 (1H, t, *J* 6.4 Hz, NH), 9.29 (1H, s, phenyl-OH), 9.77 (1H, br s, NH), 10.38 (1H, br s, OH). δ_C (75.46 MHz, DMSO-d_6) 33.6, 42.3, 115.1, 128.2, 129.6, 155.9, 158.1 (C=NOH). *m/z* (ESI^+) 196 $[M + H]^+$.

N-2-(2′-Methoxyphenyl)ethyl-N′-hydroxyguanidine Hydrochloride ***1n***. Colorless crystals (46%). Found: C, 49.02; H, 6.62; N, 17.11%. $C_{10}H_{16}ClN_3O_2$ requires C, 48.88 H, 6.56; N, 17.10%. δ_H (300 MHz, DMSO-d_6) 2.78 (2H, t, *J* 7.2 Hz, CH_2-2), 3.28−3.36 (2H, m, CH_2-1), 3.78 (3H, s, OCH_3), 6.84−6.99 (2H, m, H-3′, 5′), 7.17−7.25 (2H, m, H-4′,6′), 7.65 (2H, br s, NH_2), 7.85 (1H, t, *J* 5.8 Hz, NH), 9.79 (1H, br s, NH), 10.38 (1H, br s, OH). δ_C (75.46 MHz, DMSO-d_6) 28.9, 40.7, 55.3, 110.6, 120.2, 126.0, 127.9, 130.1, 157.1, 158.2 (C=NOH). *m/z* (ESI^+), 210 $[M + H]^+$.

N-2-(3′-Methoxyphenyl)ethyl-N′-hydroxyguanidine Hydrochloride ***1p***. Colorless solid (53%). Found: C, 48.10; H, 6.65; N, 17.01%. $C_{10}H_{16}ClN_3O_2{\cdot}0.2H_2O$ requires C, 48.18; H, 6.63; N, 16.85%. δ_H (300 MHz, DMSO-d_6) 2.76 (2H, t, *J* 7.2 Hz, H-2), 3.38−3.43 (2H, m, H-1), 3.74 (3H, s, OCH_3), 6.75−6.89 (3H, m, H-2′, 4′, 6′), 7.21 (1H, t, *J* 8.4 Hz, H-5′), 7.72 (2H, br s, NH_2), 7.92 (1H, t, *J* 5.9 Hz, NH), 9.84 (1H, br s, NH), 10.29 (1H, br s, OH). δ_C (75.46 MHz, DMSO-d_6) 34.9, 42.2, 55.3, 112.3, 114.8, 121.4, 129.7, 140.21, 158.5 (C=NOH), 159.6. *m/z* (ESI^+) 210 $[M + H]^+$.

N-2-(4′-Methoxyphenyl)ethyl-N′-hydroxyguanidine Hydrochloride ***1q***. Colorless crystals (58%). Found: C, 49.16; H, 6.24; N, 16.89%. $C_{10}H_{16}ClN_3O_2$ requires C, 48.88; H, 6.56; N, 17.10%. δ_H (300 MHz, DMSO-d_6) 2.72 (2H, t, *J* 7.2 Hz, CH_2-2), 3.30−3.38 (2H, m, CH_2-1), 3.72 (3H, s, OCH_3), 6.83−6.89 (2H, m, H-3′, 5′), 7.16−7.22 (2H, m, H-2′,6′), 7.69 (2H, br s, NH_2), 7.89 (1H, t, *J* 5.8 Hz, NH), 9.83 (1H, br s, NH), 10.45 (1H, br s, OH). δ_C (75.46 MHz, DMSO-d_6) 34.1, 42.6, 55.4, 114.1, 130.2, 130.7, 157.8, 158.1 (C=NOH); *m/z* (ESI^+), 210 $[M + H]^+$.

N-2-(1′-Naphthyl)ethyl-N′-hydroxyguanidine Hydrochloride ***1r***. Off-white solid (79%). Found: C, 58.47; H, 6.14; N, 15.86%. $C_{13}H_{16}ClN_3O$ requires C, 58.76; H, 6.07; N, 15.81%. δ_H (300 MHz, DMSO-d_6) 3.24−3.32 (2H, m, CH_2-1), 3.45−3.55 (2H, m, CH_2-2), 7.36−7.46 (2H, m, H-6′, 7′), 7.43−7.56 (2H, m, H-2′, 3′), 7.73 (2H, br s, NH_2), 7.82 (1H, m, H-5′), 7.94 (1H, d, *J* 8.4 Hz, H-8′), 8.05 (1H, br t, *J* 6.2 Hz, NH), 9.85 (1H, br s, NH), 10.46 (1H, br s, OH). δ_C (75.46 MHz, DMSO-d_6) 31.5, 41.3, 123.6, 125.5, 125.7, 126.2, 126.9, 127.1, 128.6, 131.4, 133.4, 134.2, 158.1 (C=NOH). *m/z* (ESI^+) 230 $[M + H]^+$.

N-2-(4′-Sulfamoylphenyl)ethyl-N′-hydroxyguanidine Hydrochloride ***1s***. Colorless solid (21%); Found: C, 37.00; H, 5.32; N, 18.69%. $C_9H_{15}ClN_4O_3S$ requires C, 36.67; H, 5.13; N, 19.01%. δ_H (300 MHz,

dx.doi.org/10.1021/jm400146r | J. Med. Chem. XXXX, XXX, XXX−XXX

DMSO-d_6) 2.87 (2H, t, J 7 Hz, CH_2-2), 3.36−3.47 (2H, m, CH_2-1), 7.32 (2H, br s, NH_2), 7.42−7.48 (2H, m, H-2′, 6′), 7.69 (2H, br s, NH_2), 7.73−7.79 (2H, m, H-3′, 5′), 7.87 (1H, br s, NH), 9.75 (1H, br s, NH/OH), 10.34 (1H, br s, NH/OH). δ_C (75.46 MHz, DMSO-d_6) 34.6, 42.0, 126.1, 129.7, 142.8, 142.9, 158.6 (C═NOH). m/z (ESI^+) 259 $[M + H]^+$.

N-Phenethyl-N′-GlugGABAoxy-N″-GluGABAguanidine **9**.[54] Colorless powder (47%). Found: C, 53.43; H, 6.65; N, 15.97%. $C_{27}H_{41}N_7O_9$ requires C, 53.37; H, 6.80; N, 16.14%. δ_H (300 MHz, D_2O) 1.79−1.64 (m, 4H, 2 × GABA-β), 2.05−1.94 (m, 4H, 2 × Glu-β), 2.45−2.22 (m, 8H, 2 × GABA-α + 2 × Glu-γ), 2.69 (t, 1H, J 6.5 Hz, 1/2 CH_2-2), 2.81 (t, 1H, J 6.5 Hz, 1/2 CH_2-2), 3.15 −3.06 (m, 4H, 2 × GABA-γ CH_2), 3.29 (dt, 2H, J 9.4, 6.6 Hz, CH_2-1), 3.66−3.60 (m, 2H, 2 × Glu-α), 7.30−7.07 (m, 5H, PhH). δ_C ($CDCl_3$, 100 MHz) 23.8, 23.9, 24.1, 26.4, 29.8, 31.5, 33.7, 36.3, 38.5, 42.0, 42.4, 43.6, 54.1, 126.6, 128.7, 129.0, 138.8, 173.2 (overlapped), 173.9, 174.6. m/z (ESI^+) 608 $[M + H]^+$. m/z (ESI^-) 606 $[M - H]^-$.

N-Phenethyl-N′-(4-(γ-glutamylamino))benzyloxyguanidine **10**.[54] Colorless solid (0.150 g, 74%). Purity was 98% according to HPLC analysis. δ_H (D_2O, 300 MHz) 2.16 (q, 2H, J 7.4 Hz, Glu-β), 2.60−2.54 (m, 2H, Glu-γ), 2.69 (t, 2H, J 6.6 Hz, CH_2-2), 3.32 (t, 2H, J 6.6 Hz, CH_2-1), 3.74 (t, 1H, J 6.2 Hz, Glu-α), 4.75 (s, 2H, CH_2), 7.11 (d, 2H, J 8.2 Hz, Ar H), 7.48−7.24 (m, 7H, Ar H). δ_C (62.5 MHz, DMSO-d_6), 27.6, 33.5, 35.8, 42.9, 54.1, 74.4, 119.2, 126.5, 128.8, 129.0, 129.2, 133.7, 138.5, 140.0, 154.8, 170.0, 170.8. m/z (ESI^+) 414 $[M + H]^+$.

Biological Assessment. *Animals.* The animal care and experimental procedures were in accordance with the United Kingdom Animal (Scientific Procedures) Act, 1986. Male Wistar rats weighing between 250 and 450 g were used in all animal experiments.

In Vitro NO_x Analysis. Stock solutions of X/XO, γ-GT/gly-gly were made fresh on each experimental day in KPE buffer. Crude homogenates of rat liver, renal medulla, and renal cortex were prepared in ice-cold HBSS containing 1% Triton X from freshly killed adult male Wistar rats using a mechanical homogenizer and sonicator bath. NHGs (100 μM) were added to enzyme preparations (100 μM X/100 mU XO and 100 mU γ-GT/5 mM gly-gly) or tissue homogenates with and without the relevant inhibitors (5-sulfosalicylic acid (100 μM) for γ-GT; allopurinol for XO (100 μM) and L-NAME (200 μM) for NOS in homogenates for (1 h, 37 °C), before samples were centrifuged (1000g; 4 °C) and NO_x assayed using the Griess test (R&D Systems). This test does not measure NO directly, but measures $[NO_2^- + NO_3^-]$ as a surrogate of NO.

Vasodilator Experiments. Rings (∼3 mm) of rat aorta were mounted in a myograph (Danish Myo model 703, 37 °C) containing Krebs buffer solution (composition mM: NaCl 118, KCl 4.7, $CaCl_2$ 2.5, $MgSO_4$ 1.2, KH_2PO_4 1.2, $NaHCO_3$ 35, glucose 10), oxygenated with 95% O_2, 5% CO_2. Vascular rings were stretched to 15 mN over a 1 h period, and the maximal contraction determined by replacing standard Krebs buffer solution with Krebs containing 60 mM KCl. Subsequently, aortic rings were precontracted to ∼80% of the KCl-induced maximal contraction with phenylephrine (PE 10−300 nM) prior to confirmation of endothelial integrity using the endothelium-dependent vasodilator, acetylcholine (ACh; 10 μM). Relaxation of >80% was considered to confirm functional integrity of the endothelium and rings that failed to relax to this extent were rejected. Following washout of ACh, precontracted rings were either treated with NHGs (100 μM, single exposure in preliminary experiments or cumulative concentrations of 1−100 μM in subsequent characterization experiments). Parallel rings were incubated with L-NAME (200 μM), L-Arg (100 μM), hemoglobin (10 μM), or ODQ (50 μM) prior to and during exposure to ACh, NOHA, and NHG analogues to determine whether the compounds acted independently of NOS, compete with L-Arg for cellular uptake, generate NO that is scavenged by hemoglobin, or act via sGC activation, respectively. In some experiments involving prodrugs, glutamyl-linked NHGs (10 mM) were preincubated with γ-GT (100 mU/5 mM gly-gly; 1h, 37 °C) prior to addition to the myograph.

Isolated Perfused Kidney. The isolated perfused kidney preparation was performed as previously described.[75] Briefly, rats were anaesthetized by intraperitoneal injection with sodium pentobarbital (60 mg/kg body weight) prior to heparinization (500 U). A midline laparotomy incision was made from pelvis to sternum, exposing the abdominal cavity. A cannula was inserted into the renal artery via the superior mesenteric artery and tied in place. Perfusion with a modified Krebs−Henseleit solution (containing 6.7% bovine serum albumin and 20 amino acids) commenced immediately, with a view to minimizing renal hypoxia. The right kidney and ureter were dissected free and transferred to a temperature controlled moisture chamber (Harvard 834/8; Harvard Apparatus) and perfused with 40 mL of recirculating perfusate at a constant rate of 10 mL/min via a peristaltic roller pump (Gilson miniplus 3). Perfusion pressure was measured via a side port and transducer, with 10 mL/min perfusion inducing a pressure of 60.6 ± 2.9 mmHg. Following equilibration (20 min), the kidney vasculature was constricted by addition of the α_1-adrenoceptor agonist, PE (0.3 μM incremental additions), until perfusion pressure reached 120−140 mmHg. Cumulative concentrations of **1e**, **9**, and **10** (1 μM to 1 mM) were added to the perfusate to assess the impact of these compounds on renal perfusion.

Renal Prodrug Activation. The selected candidate prodrug **10** was incubated at three concentrations (1, 10, and 100 μM) with freshly pooled (n = 3) male rat (Wistar) kidney homogenates and samples taken at 15 min intervals over a 45 min incubation period for LC-MS/MS analysis (Quattro Micro Mass Spectrometer, Micromass, UK; positive ion mode, Phenomenex Luna 2.5 μm C18 column, mobile phase 0.1% formic acid in 95% water, 5% acetonitrile). Total protein concentrations were determined by Lowry assay.

Statistical Analysis. All data are expressed as mean ± SEM. Statistical analysis of NO_x data was conducted using paired Student t-tests. Comparisons of vasodilator effects were conducted using Student's t-tests or one-way ANOVAs followed by Dunnett's post-tests, as appropriate, while those for concentration−response curves was performed using 2-way ANOVA, followed by Bonferroni post-tests. $P < 0.05$ was considered to be significant (analysis conducted using Graphpad Prism 5.00).

■ ASSOCIATED CONTENT

Ⓢ Supporting Information

Preparation and characterization of compound **1b**, **3**, **4**, **5**, **8**; ^1H NMR and 2D $^1H-^{13}C$ HMBC spectra of *N*-(4-phenylbutyl)-*N*′-hydroxyguanidine **1g** in DMSO-d_6; HPLC traces of **9** and **10**. This material is available free of charge via the Internet at http://pubs.acs.org

■ AUTHOR INFORMATION

Corresponding Author

*Phone: +44 (0)1463 279562. Fax: +44 (0)1463 711245. E-mail: ian.megson@uhi.ac.uk.

Author Contributions

All authors contributed to the writing of this manuscript and approved the final version.

Notes

The authors declare no competing financial interest.

†Nigel P. Botting died 4 June 2011.

■ ACKNOWLEDGMENTS

We thank the Wellcome Trust for supporting this research (Catalyst Biomedica, Translational Award 063729/Z/01/Z).

■ ABBREVIATIONS USED[a]

ACh, acetylcholine; ARF, acute renal failure; γ-GT, γ-glutamyl transpeptidase; Hb, hemoglobin; NHG, *N*-hydroxyguanidine; NOHA, *N*-hydroxyarginine; NO, nitric oxide; NOx, [nitrite + nitrate]; NOS, NO synthase; L-NAME, N^{ω}-nitro-L-arginine methyl ester; ODQ, 1*H*-[1,2,4]oxadiazolo[4, 3-*a*]quinoxalin-1-one; ROS, reactive oxygen species; X, xanthine; XO, xanthine

oxidase; Fm, (9-fluorenyl)methyl; Fmoc, (9-fluorenyl)-methoxycarbonyl; GABA, γ-aminobutanoyl; Glu, γ-glutamyl; glygly, glycylglycine; EDC, 1-ethyl-3-(3-dimethylaminopropyl)-carbodiimide; HOBt, *N*-hydroxybenzotriazole hydrate; $(Boc)_2O$, di-*tert*-butyl dicarbonate; Boc, *tert*-butoxycarbonyl; TsOH, *p*-toluenesulfonic acid; DMSO, dimethyl sulfoxide; DMF, dimethylformamide; Et_3N, triethylamine; DCM, dichloromethane; HBSS, Hanks-balanced saline solution; KPE, potassium phosphate-EDTA; LC-MS/MS, liquid chromatography mass spectrometry; PE, phenylephrine hydrochloride

■ ADDITIONAL NOTE

[a]Abbreviations for common amino acids are in accordance with the recommendations of IUPAC.

■ REFERENCES

(1) Groeneveld, A. B.; Tran, D. D.; van der Meulen, J.; Nauta, J. J.; Thijs, L. G. Acute renal failure in the medical intensive care unit: predisposing, complicating factors and outcome. *Nephron* **1991**, *59*, 602−610.

(2) Levy, E. M.; Viscoli, C. M.; Horwitz, R. I. The effect of acute renal failure on mortality. A cohort analysis. *JAMA, J. Am. Med. Assoc.* **1996**, *275*, 1489−1494.

(3) Bagshaw, S. M. The long-term outcome after acute renal failure. *Curr. Opin. Crit. Care* **2006**, *12*, 561−566.

(4) Hilton, R. Acute renal failure. *BMJ (Br. Med. J.)* **2006**, *333*, 786−790.

(5) Gelman, S. The pathophysiology of aortic cross-clamping and unclamping. *Anesthesiology* **1995**, *82*, 1026−1060.

(6) Grun, R. P.; Constantinovici, N.; Normand, C.; Lamping, D. L. Costs of dialysis for elderly people in the UK. *Nephrol., Dial., Transplant.* **2003**, *18*, 2122−2127.

(7) Chertow, G. M.; Sayegh, M. H.; Allgren, R. L.; Lazarus, J. M. Is the administration of dopamine associated with adverse or favorable outcomes in acute renal failure? Auriculin Anaritide Acute Renal Failure Study Group. *Am. J. Med.* **1996**, *101*, 49−53.

(8) Lassnigg, A.; Donner, E.; Grubhofer, G.; Presterl, E.; Druml, W.; Hiesmayr, M. Lack of renoprotective effects of dopamine and furosemide during cardiac surgery. *J. Am. Soc. Nephrol.* **2000**, *11*, 97−104.

(9) Bellomo, R.; Chapman, M.; Finfer, S.; Hickling, K.; Myburgh, J. Low-dose dopamine in patients with early renal dysfunction: a placebo-controlled randomised trial. Australian and New Zealand Intensive Care Society (ANZICS) Clinical Trials Group. *Lancet* **2000**, *356*, 2139−2143.

(10) Takala, J.; Meier-Hellmann, A.; Eddleston, J.; Hulstaert, P.; Sramek, V. Effect of dopexamine on outcome after major abdominal surgery: a prospective, randomized, controlled multicenter study. European Multicenter Study Group on Dopexamine in Major Abdominal Surgery. *Crit. Care Med.* **2000**, *28*, 3417−3423.

(11) Dehne, M. G.; Klein, T. F.; Muhling, J.; Sablotzki, A.; Osmer, C.; Hempelmann, G. Impairment of renal function after cardiopulmonary bypass is not influenced by dopexamine. *Renal Failure* **2001**, *23*, 217−230.

(12) Ralph, C. J.; Tanser, S. J.; Macnaughton, P. D.; Sinclair, D. G. A randomised controlled trial investigating the effects of dopexamine on gastrointestinal function and organ dysfunction in the critically ill. *Intensive Care Med.* **2002**, *28*, 884−890.

(13) Kellum, J. A. Use of diuretics in the acute care setting. *Kidney Int., Suppl.* **1998**, *66*, S67−70.

(14) Dorman, H. R.; Sondheimer, J. H.; Cadnapaphornchai, P. Mannitol-induced acute renal failure. *Medicine (Baltimore)* **1990**, *69*, 153−159.

(15) Mehta, R. L.; Pascual, M. T.; Soroko, S.; Chertow, G. M. Diuretics, mortality, and nonrecovery of renal function in acute renal failure. *JAMA, J. Am. Med. Assoc.* **2002**, *288*, 2547−2553.

(16) Ladefoged, S. D.; Andersen, C. B. Calcium channel blockers in kidney transplantation. *Clin. Transplant.* **1994**, *8*, 128−133.

(17) Allgren, R. L.; Marbury, T. C.; Rahman, S. N.; Weisberg, L. S.; Fenves, A. Z.; Lafayette, R. A.; Sweet, R. M.; Genter, F. C.; Kurnik, B. R.; Conger, J. D.; Sayegh, M. H. Anaritide in acute tubular necrosis. Auriculin Anaritide Acute Renal Failure Study Group. *N. Engl. J. Med.* **1997**, *336*, 828−834.

(18) Briguori, C.; Manganelli, F.; Scarpato, P.; Elia, P. P.; Golia, B.; Riviezzo, G.; Lepore, S.; Librera, M.; Villari, B.; Colombo, A.; Ricciardelli, B. Acetylcysteine and contrast agent-associated nephrotoxicity. *J. Am. Coll. Cardiol.* **2002**, *40*, 298−303.

(19) Durham, J. D.; Caputo, C.; Dokko, J.; Zaharakis, T.; Pahlavan, M.; Keltz, J.; Dutka, P.; Marzo, K.; Maesaka, J. K.; Fishbane, S. A randomized controlled trial of *N*-acetylcysteine to prevent contrast nephropathy in cardiac angiography. *Kidney Int.* **2002**, *62*, 2202−2207.

(20) Schneider, R.; Raff, U.; Vornberger, N.; Schmidt, M.; Freund, R.; Reber, M.; Schramm, L.; Gambaryan, S.; Wanner, C.; Schmidt, H. H.; Galle, J. L-Arginine counteracts nitric oxide deficiency and improves the recovery phase of ischemic acute renal failure in rats. *Kidney Int.* **2003**, *64*, 216−225.

(21) Gryglewski, R. J.; Palmer, R. M.; Moncada, S. Superoxide anion is involved in the breakdown of endothelium-derived vascular relaxing factor. *Nature* **1986**, *320*, 454−456.

(22) MacKenzie, A.; Martin, W. Loss of endothelium-derived nitric oxide in rabbit aorta by oxidant stress: restoration by superoxide dismutase mimetics. *Br. J. Pharmacol.* **1998**, *124*, 719−728.

(23) Conger, J.; Robinette, J.; Villar, A.; Raij, L.; Shultz, P. Increased nitric oxide synthase activity despite lack of response to endothelium-dependent vasodilators in postischemic acute renal failure in rats. *J. Clin. Invest.* **1995**, *96*, 631−638.

(24) Kakoki, M.; Hirata, Y.; Hayakawa, H.; Suzuki, E.; Nagata, D.; Tojo, A.; Nishimatsu, H.; Nakanishi, N.; Hattori, Y.; Kikuchi, K.; Nagano, T.; Omata, M. Effects of tetrahydrobiopterin on endothelial dysfunction in rats with ischemic acute renal failure. *J. Am. Soc. Nephrol.* **2000**, *11*, 301−309.

(25) Chirino, Y. I.; Hernandez-Pando, R.; Pedraza-Chaverri, J. Peroxynitrite decomposition catalyst ameliorates renal damage and protein nitration in cisplatin-induced nephrotoxicity in rats. *BMC Pharmacol.* **2004**, *4*, 20.

(26) Bech, J. N.; Nielsen, C. B.; Pedersen, E. B. Effects of systemic NO synthesis inhibition on RPF, GFR, UNa, and vasoactive hormones in healthy humans. *Am. J. Physiol.* **1996**, *270*, F845−F851.

(27) Pararajasingam, R.; Weight, S. C.; Bell, P. R.; Nicholson, M. L.; Sayers, R. D. Prevention of renal impairment following aortic cross-clamping by manipulation of the endogenous renal nitric oxide response. *Eur. J. Vasc. Endovasc. Surg.* **2000**, *19*, 396−399.

(28) Chintala, M. S.; Chiu, P. J.; Vemulapalli, S.; Watkins, R. W.; Sybertz, E. J. Inhibition of endothelial derived relaxing factor (EDRF) aggravates ischemic acute renal failure in anesthetized rats. *Naunyn-Schmiedeberg's Arch. Pharmacol.* **1993**, *348*, 305−310.

(29) Mashiach, E.; Sela, S.; Winaver, J.; Shasha, S. M.; Kristal, B. Renal ischemia-reperfusion injury: contribution of nitric oxide and renal blood flow. *Nephron* **1998**, *80*, 458−467.

(30) Matsumura, Y.; Nishiura, M.; Deguchi, S.; Hashimoto, N.; Ogawa, T.; Seo, R. Protective effect of FK409, a spontaneous nitric oxide releaser, on ischemic acute renal failure in rats. *J. Pharmacol. Exp Ther.* **1998**, *287*, 1084−1091.

(31) Kurata, H.; Takaoka, M.; Kubo, Y.; Katayama, T.; Tsutsui, H.; Takayama, J.; Matsumura, Y. Nitric Oxide Protects against Ischemic Acute Renal Failure through the Suppression of Renal Endothelin-1 Overproduction. *J. Cardiovasc. Pharmacol.* **2004**, *44* (Suppl 1), S455−S458.

(32) Wilhelm, S. M.; Simonson, M. S.; Robinson, A. V.; Stowe, N. T.; Schulak, J. A. Endothelin up-regulation and localization following renal ischemia and reperfusion. *Kidney Int.* **1999**, *55*, 1011−1018.

(33) Miller, M. R.; Megson, I. L. Recent developments in nitric oxide donor drugs. *Br. J. Pharmacol.* **2007**, *151*, 305−321.

(34) Renodon-Corniere, A.; Dijols, S.; Perollier, C.; Lefevre-Groboillot, D.; Boucher, J. L.; Attias, R.; Sari, M. A.; Stuehr, D.;

Mansuy, D. *N*-Aryl *N*′-hydroxyguanidines, a new class of NO-donors after selective oxidation by nitric oxide synthases: structure−activity relationship. *J. Med. Chem.* **2002**, *45*, 944−954.
(35) Mansuy, D.; Boucher, J. L. Alternative nitric oxide-producing substrates for NO synthases. *Free Radical Biol. Med.* **2004**, *37*, 1105−1121.
(36) Boucher, J. L.; Genet, A.; Vadon, S.; Delaforge, M.; Henry, Y.; Mansuy, D. Cytochrome P450 catalyzes the oxidation of *N*-omega-hydroxy-L-arginine by NADPH and O_2 to nitric oxide and citrulline. *Biochem. Biophys. Res. Commun.* **1992**, *187*, 880−886.
(37) Boucher, J. L.; Genet, A.; Vadon, S.; Delaforge, M.; Mansuy, D. Formation of nitrogen oxides and citrulline upon oxidation of *N*-omega-hydroxy-L-arginine by hemeproteins. *Biochem. Biophys. Res. Commun.* **1992**, *184*, 1158−1164.
(38) Dambrova, M.; Uhlen, S.; Welch, C. J.; Wikberg, J. E. Identification of an *N*-hydroxyguanidine reducing activity of xanthine oxidase. *Eur. J. Biochem.* **1998**, *257*, 178−184.
(39) Barthelmebs, M.; Caillette, A.; Ehrhardt, J. D.; Velly, J.; Imbs, J. L. Metabolism and vascular effects of gamma-L-glutamyl-L-dopa on the isolated rat kidney. *Kidney Int.* **1990**, *37*, 1414−1422.
(40) Wilk, S.; Mizoguchi, H.; Orlowski, M. gamma-Glutamyl dopa: a kidney-specific dopamine precursor. *J. Pharmacol. Exp. Ther.* **1978**, *206*, 227−232.
(41) Li Kam Wa, T. C.; Freestone, S.; Samson, R. R.; Johnston, N. R.; Lee, M. R. Renal metabolism and effects of the glutamyl derivatives of L-dopa and 5-hydroxytryptophan in man. *Clin. Sci.* **1996**, *91*, 177−185.
(42) Worth, D. P.; Harvey, J. N.; Brown, J.; Lee, M. R. gamma-L-Glutamyl-L-dopa is a dopamine pro-drug, relatively specific for the kidney in normal subjects. *Clin. Sci.* **1985**, *69*, 207−214.
(43) Rosalki, S. B. gamma-Glutamyl transpeptidase. *Adv. Clin. Chem.* **1975**, *17*, 53−107.
(44) Tate, S. S.; Meister, A. gamma-Glutamyl transpeptidase: catalytic, structural and functional aspects. *Mol. Cell. Biochem.* **1981**, *39*, 357−368.
(45) Jia, Q.; Cai, T.; Huang, M.; Li, H.; Xian, M.; Poulos, T. L.; Wang, P. G. Isoform-selective substrates of nitric oxide synthase. *J. Med. Chem.* **2003**, *46*, 2271−2274.
(46) Pufahl, R. A.; Nanjappan, P. G.; Woodard, R. W.; Marletta, M. A. Mechanistic probes of *N*-hydroxylation of L-arginine by the inducible nitric oxide synthase from murine macrophages. *Biochemistry* **1992**, *31*, 6822−6828.
(47) Wagenaar, F. L.; Kerwin, J. F. Methodology for the Preparation of *N*-Guanidino-Modified Arginines and Related Derivatives. *J. Org. Chem.* **1993**, *58*, 4331−4338.
(48) Wallace, G. C.; Fukuto, J. M. Synthesis and bioactivity of *N*-omega-hydroxyarginine: a possible intermediate in the biosynthesis of nitric oxide from arginine. *J. Med. Chem.* **1991**, *34*, 1746−1748.
(49) Xian, M.; Fujiwara, N.; Wen, Z.; Cai, T. W.; Kazuma, S.; Janczuk, A. J.; Tang, X. P.; Telyatnikov, V. V.; Zhang, Y. X.; Chen, X. C.; Miyamoto, Y.; Taniguchi, N.; Wang, P. G. Novel substrates for nitric oxide synthases. *Bioorg. Med. Chem.* **2002**, *10*, 3049−3055.
(50) Xian, M.; Li, X. P.; Tang, X. P.; Chen, X. C.; Zheng, X. L.; Galligan, J. J.; Kreulen, D. L.; Wang, P. G. *N*-Hydroxyl derivatives of guanidine based drugs as enzymatic NO donors. *Bioorg. Med. Chem. Lett.* **2001**, *11*, 2377−2380.
(51) Caddick, S.; Judd, D. B.; Lewis, A. K. D.; Reich, M. T.; Williams, M. R. V. A generic approach for the catalytic reduction of nitriles. *Tetrahedron* **2003**, *59*, 5417−5423.
(52) Zani, B. G.; Bohlen, H. G. Transport of extracellular L-arginine via cationic amino acid transporter is required during in vivo endothelial nitric oxide production. *American J. Physiol: Heart Circul. Physiol.* **2005**, *289*, H1381−H1390.
(53) Zharikov, S. I.; Block, E. R. Characterization of L-arginine uptake by plasma membrane vesicles isolated from cultured pulmonary artery endothelial cells. *Biochim. Biophys. Acta* **1998**, *1369*, 173−183.
(54) Zhang, Q.; Megson, I.; Botting, N. P.; Webb, D. J.; Kulczynska, A. A new class of NO-donor pro-drugs triggered by [gamma]-glutamyl transpeptidase with potential for reno-selective vasodilatation. *Chem. Commun.* **2012**, *49*, 1389−1391.
(55) Leenders, R. G. G.; Gerrits, K. A. A.; Ruijtenbeek, R.; Scheeren, H. W.; Haisma, H. J.; Boven, E. beta-Glucuronyl Carbamate Based Pro-Moieties Designed for Prodrugs in Adept. *Tetrahedron Lett.* **1995**, *36*, 1701−1704.
(56) Menard, A.; Castonguay, R.; Lherbet, C.; Rivard, C.; Roupioz, Y.; Keillor, J. W. Nonlinear free energy relationship in the general-acid-catalyzed acylation of rat kidney gamma-glutamyl transpeptidase by a series of gamma-glutamyl anilide substrate analogues. *Biochemistry* **2001**, *40*, 12678−12685.
(57) Thompson, G. A.; Meister, A. Interrelationships between Binding-Sites for Amino-Acids, Dipeptides, and Gamma-Glutamyl Donors in Gamma-Glutamyl Transpeptidase. *J. Biol. Chem.* **1977**, *252*, 6792−6798.
(58) Tate, S. S.; Meister, A. Gamma-Glutamyl-Transferase Transpeptidase from Kidney. *Methods Enzymol.* **1985**, *113*, 400−419.
(59) Elsadek, B.; Graeser, R.; Warnecke, A.; Unger, C.; Saleem, T.; El-Melegy, N.; Madkor, H.; Kratz, F. Optimization of an Albumin-Binding Prodrug of Doxorubicin That Is Cleaved by Prostate-Specific Antigen. *Med. Chem. Lett.* **2010**, *1*, 234−238.
(60) Antczak, C.; Bauvois, B.; Monneret, C.; Florent, J. C. A new acivicin prodrug designed for tumor-targeted delivery. *Bioorg. Med. Chem.* **2001**, *9*, 2843−2848.
(61) de Groot, F. M. H.; Loos, W. J.; Koekkoek, R.; van Berkom, L. W. A.; Busscher, G. F.; Seelen, A. E.; Albrecht, C.; de Bruijn, P.; Scheeren, H. W. Elongated multiple electronic cascade and cyclization spacer systems in activatible anticancer prodrugs for enhanced drug release. *J. Org. Chem.* **2001**, *66*, 8815−8830.
(62) de Groot, F. M. H.; van Berkom, L. W. A.; Scheeren, H. W. Synthesis and biological evaluation of 2′-carbamate-linked and 2′-carbonate-linked prodrugs of paclitaxel: selective activation by the tumor-associated protease plasmin. *J. Med. Chem.* **2000**, *43*, 3093−3102.
(63) Elsadek, B.; Graeser, R.; Esser, N.; Schafer-Obodozie, C.; Abu Ajaj, K.; Unger, C.; Warnecke, A.; Saleem, T.; El-Melegy, N.; Madkor, H.; Kratz, F. Development of a novel prodrug of paclitaxel that is cleaved by prostate-specific antigen: an in vitro and in vivo evaluation study. *Eur. J. Cancer* **2010**, *46*, 3434−3444.
(64) Fossey, C.; Huynh, N. T.; Vu, A. H.; Vidu, A.; Zarafu, I.; Laduree, D.; Schmidt, S.; Laumond, G.; Aubertin, A. M. Synthesis and anti-HIV evaluation of hybrid-type prodrugs conjugating HIV integrase inhibitors with d4t by self-cleavable spacers containing an amino acid residue. *J. Enzyme Inhib. Med. Chem.* **2007**, *22*, 608−619.
(65) Greenwald, R. B.; Pendri, A.; Conover, C. D.; Zhao, H.; Choe, Y. H.; Martinez, A.; Shum, K.; Guan, S. Y. Drug delivery systems employing 1,4-or 1,6-elimination: poly(ethylene glycol) prodrugs of amine-containing compounds. *J. Med. Chem.* **1999**, *42*, 3657−3667.
(66) Hay, M. P.; Wilson, W. R.; Denny, W. A. Nitroarylmethylcarbamate prodrugs of doxorubicin for use with nitroreductase gene-directed enzyme prodrug therapy. *Bioorg. Med. Chem.* **2005**, *13*, 4043−4055.
(67) Muller, I. A.; Kratz, F.; Jung, M.; Warnecke, A. Schiff bases derived from *p*-aminobenzyl alcohol as trigger groups for pH-dependent prodrug activation. *Tetrahedron Lett.* **2010**, *51*, 4371−4374.
(68) Niculescu-Duvaz, D.; Heyes, J.; Springer, C. J. Structure−activity relationship in cationic lipid mediated gene transfection. *Curr. Med. Chem.* **2003**, *10*, 1233−1261.
(69) You, H.; Yoon, H. E.; Yoon, J. H.; Ko, H.; Kim, Y. C. Synthesis of pheophorbide-a conjugates with anticancer drugs as potential cancer diagnostic and therapeutic agents. *Bioorg. Med. Chem.* **2011**, *19*, 5383−5391.
(70) Lefevre-Groboillot, D.; Boucher, J. L.; Stuehr, D. J.; Mansuy, D. Relationship between the structure of guanidines and *N*-hydroxyguanidines, their binding to inducible nitric oxide synthase (iNOS) and their iNOS-catalysed oxidation to NO. *FEBS J.* **2005**, *272*, 3172−3183.
(71) Slama, P.; Boucher, J. L.; Reglier, M. Aromatic *N*-hydroxyguanidines as new reduction cosubstrates for dopamine beta-hydroxylase. *Biochem. Biophys. Res. Commun.* **2004**, *316*, 1081−1087.

(72) Moali, C.; Boucher, J. L.; Renodon-Corniere, A.; Stuehr, D. J.; Mansuy, D. Oxidations of *N*(omega)-hydroxyarginine analogues and various *N*-hydroxyguanidines by NO synthase II: key role of tetrahydrobiopterin in the reaction mechanism and substrate selectivity. *Chem. Res. Toxicol.* **2001**, *14*, 202−210.
(73) Beranova, P.; Chalupsky, K.; Kleschyov, A. L.; Schott, C.; Boucher, J. L.; Mansuy, D.; Munzel, T.; Muller, B.; Stoclet, J. C. *N*-omega-hydroxy-L-arginine homologues and hydroxylamine as nitric oxide-dependent vasorelaxant agents. *Eur. J. Pharmacol.* **2005**, *516*, 260−267.
(74) McDonald, K. K.; Rouhani, R.; Handlogten, M. E.; Block, E. R.; Griffith, O. W.; Allison, R. D.; Kilberg, M. S. Inhibition of endothelial cell amino acid transport system y+ by arginine analogs that inhibit nitric oxide synthase. *Biochim. Biophys. Acta* **1997**, *1324*, 133−141.
(75) De Mello, G.; Maack, T. Nephron function of the isolated perfused rat kidney. *Am. J. Physiol.* **1976**, *231*, 1699−1707.

dx.doi.org/10.1021/jm400146r | *J. Med. Chem.* XXXX, XXX, XXX−XXX